Applied Acoustics 143 (2019) 151–156

Contents lists available at ScienceDirect

Applied Acoustics

journal homepage: www.elsevier.com/locate/apacoust

Acoustic gradient surfaces and gradient-index surfaces: Principles and applications on noise control

Xu Wang [a,b], Wuzhou Yu [a], Zaixiu Jiang [a], Xiaonan Wang [c,*], Dongxing Mao [a,*]

[a] Institute of Acoustics, School of Physics Science and Engineering, Tongji University, No. 1239 Siping Road, Shanghai 200092, China
[b] College of Architecture and Urban Planning, Tongji University, No. 1239 Siping Road, Shanghai 200092, China
[c] Shanghai Academy of Environmental Sciences, No. 508 Qinzhou Road, Shanghai 200233, China

ARTICLE INFO

Article history:
Received 14 June 2018
Received in revised form 23 July 2018
Accepted 20 August 2018

ABSTRACT

Gradient surfaces (oblique reflection surfaces) and gradient-index surfaces (surfaces engraved by a series of 1/4 wavelength tubes with linearly growing length) are two solutions on manipulating the reflected sound field. For a high-rise building built close to a traffic road, implementing these two solutions in balcony ceiling design on upper floors both provide remarkable noise insertion losses. This paper presents a systematical comparison between these two surfaces, theoretically and numerically. Our results reveal their distinct underlying working mechanisms: one works by its profile (a macroscopy effect), while the other works by the multiple interferences from its distribute surface impedance (a microscopy effect). The advantage of the gradient-index surface on shielding the balcony region is further demonstrated. This paper may pave the way for the application of the gradient-index surfaces in environmental noise control.

1. Introduction

Gradient surfaces (GSs), i.e. oblique reflection surfaces, and gradient-index surfaces (GISs) are two solutions on manipulating a sound reflected field, while the latter one is recently discovered in optics and then introduced to acoustics [1,2]. The gradient-index surface here refers to a surface engraved by a series of evenly distributed 1/4 wavelength tubes in space with progressively tuned tube length. Because the phase shift of a reflected wave from a 1/4 wavelength tube is determined by the tube length, linearly growing tube lengths provide a linear local phase shift variation, i.e. a gradient phase shift. Such a surface providing a gradient phase shift is called gradient-index surface in physics. The impedance of a GIS is no longer homogeneous but shifts over the scale of a wavelength along the surface. In such cases, the reflected wave can be engineered by the impedance variation of the surface. By further introducing constant phase shift gradient, the direction of a reflected wave can be artificially tailored, which follows the generalized law of reflection [1]. Due to their great flexibility on reflected field manipulation, GISs, together with GSs, have many potential applications.

For example, it is known that when barriers are placed on opposite sides of a noise source, their performance deteriorates significantly [3]. Employing these surfaces on barrier design leads to inclined barriers and gradient-phase barriers [4–7]. These barriers work by suppressing multiple reflections between the opposite barrier walls, and both provide remarkable enhancement on shielding the surroundings.

In another case, in upper floors of a roadside building where roadside barriers cannot shield, residents usually suffer from severe traffic noise pollution. Balcony, which is regarded as one of the green architectural features, functions as a buffer zone between outdoors and indoors by providing significant noise screening even when balcony door is open for natural ventilation. However, the screening effect of a balcony was found to be significantly cancelled due to the reflection from its ceiling; in comparison, inclined ceilings [8] and gradient-phase ceilings [9–10] effectively guide the sound energy flux away from the building facade.

Although these two surface types both possess great functionality, their underlying working mechanism are distinct from each other; while a detailed comparison between these two surfaces is rarely done. This paper aims at revealing their difference on reflected field manipulation, and further exploiting their actual performance when they are implemented in noise screening applications. In Section 2, the theoretical models of these surfaces are

* Corresponding authors.
E-mail addresses: wangxn@saes.sh.cn (X. Wang), dxmao@tongji.edu.cn (D. Mao).

https://doi.org/10.1016/j.apacoust.2018.08.021
0003-682X/

conducted. Section 3 presents the strategy to suppress the thicknesses of these surfaces. Then the effects of these surfaces in noise control are compared in Section 4. Finally, conclusions are given in Section 5.

2. Theoretical modeling of GSs and GISs

Wave reflection on a gradient surface follows the Snell's law, indicating the reflected angle equals to the incident one. However, as illustrated by Fig. 1(a), by taking the normal of the ground as a reference, the relation of the incident and reflected angles with respect to the ground normal is given by

$$\theta_r - \theta_i = \alpha, \tag{1}$$

where $\alpha = 2\theta_0$ and θ_0 is the angle of tilt of the surface to the ground.

Actually, a GIS is a distributed-impedance surface, which provides local phase modulation that changes linearly along the surface. Therefore, such a surface can be realized by an array of basic acoustic structures (resonators, tubes, etc.), which are of subwavelength size and with progressively tuned geometries. Here, for example, we construct such a surface by N slender tubes with growing length as shown in Fig. 1(b), where the title angle of the envelop of the tubes end is denoted as θ_0'. Comparing Fig. 1(a) and (b) shows their differences: a GIS is achieved by engraving a serial of tubes with growing tube length on a plane, which is a slender fluted surface. In contrast, normally a GS is a slope added to a plane, resulting in a "convex" surface.

Assuming the length of the tubes in the array follows the rule $l_n = \beta x_n/2$, where x_n is the position of the nth tube in the array and β is regarded as an index related to the phase gradient of the GIS [11]. Therefore, the local phase modulation provided by nth tube should be $\phi_n = 2kl_n$, where k is the wavenumber in the air. When sound impinging on such a surface, due to the multiple interferences from the reflected wavelets from these tubes, the directivity of the reflected field is given by [11]

$$D(\theta_r) = \frac{\sin[kNd(sin\theta_r - \sin\theta_i - \beta)/2]}{N\sin[kd(sin\theta_r - \sin\theta_i - \beta)/2]} \tag{2}$$

where d is the center-to-center spacing of two nearby tubes in the array. According to Eq. (2), when the tubes array in the surface is subwavelength structured, i.e. $kd < 1$ [11], the reflected sound appears in the direction predicted by

$$\sin\theta_r - \sin\theta_i = \beta. \tag{3}$$

Eqs. (1) and (3) are the governing equations for a GS and a GIS, respectively. Intriguingly, observation of their governing equations finds their inherent relations. For a GS with a certain α, one can find a corresponding GIS with the gradient index $\beta = \sin\alpha$. This pair has many similarities: first, they reflect the normal incident sound in the same direction $\theta_r = 2\theta_0$; moreover, since the tubes on the gradient-phase surface follow the rule $l_n = \beta x_n/2$, when θ_0 is small, which is usually practical [4,6,8], one has

$$\tan\theta_0' = l_n/x_n = \sin\alpha/2 \approx \tan\theta_0. \tag{4}$$

Eq. (4) indicates that, for a GIS, the title angle of the envelop of the tubes end (θ_0') is almost the same as that of the corresponding GS (θ_0). It should be noticed that the assumption of small tilt angle is only use for deducing Eq. (4), while the performance investigation in the following of this paper apply for both small and large tilt angle cases.

In this paper, the tilt angle of the GS is set to $\theta_0 = 15°$, therefore the gradient index β of the corresponding gradient-phase surface is 1/2. By using the governing equations, Eqs. (1) and (3), the relation between the incident and reflected angles on these surfaces can be straightforwardly predicted, as illustrated by Fig. 1(c). Here the curves for the GS and the GIS are shown by the dotted and solid lines, respectively; while that for a specular reflection is given by the dashed line for comparison. Notice that the curves for the GS and GIS overlap in a wide range, indicating that for a small angle incidence, these surfaces behave identically. Therefore, it is possible to "compensate" the reflected field distortion from a complex surface profile by introducing corresponding phase index. Actually, this is the core concept of acoustical carpet cloak, a recently raised hot topic in acoustic field manipulation [12–14]. However, under large-angle incidence, as the increase of incident angle, their performances deviate from each other gradually. At last, it should be mentioned that, these results simulated at the frequency of 2000 Hz are just examples and the phenomena at other frequencies are similar, indicating the performances of both GS and GIS are dispersionless [11].

To verify the theoretical analysis above, a full wave simulation by finite element modeling using COMSOL Multiphysics is performed. The two-dimensional calculation domain is a square with side length 1 m, the investigated GS and GIS are mounted at the top; while the other sides of the calculation domain are bounded by perfectly matched layers (PMLs), which are artificial absorbing layers allowing waves to propagate out from the domain without

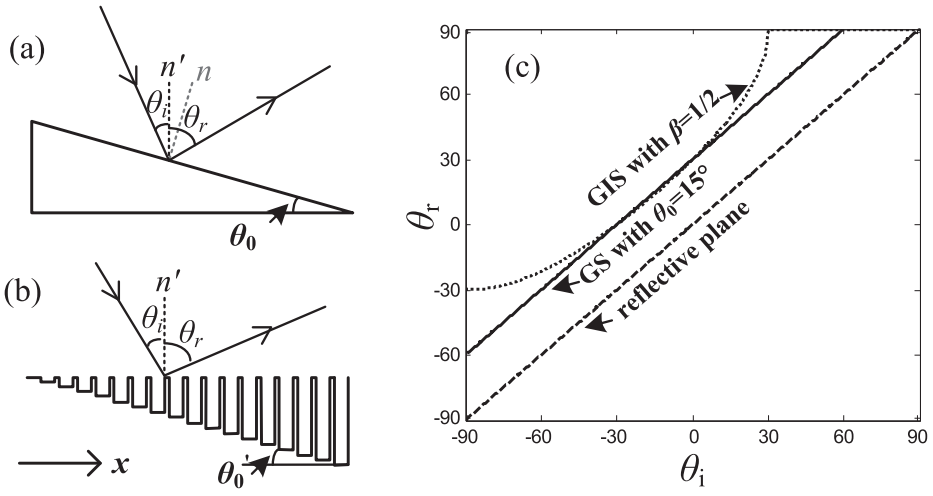

Fig. 1. Schematic diagram of wave reflection on a (a) GS and (b) GIS (n/n' denote the normal of the surface/ground); (c) relation of incident and reflected angles of the GS, GIS and plane at 2000 Hz.